American Journal of Pathology, Vol. 164, No. 2, February 2004

A Peroxisome Proliferator-Activated Receptor-α Activator Induces Renal CYP2C23 Activity and Protects from Angiotensin II-Induced Renal Injury

Dominik N. Muller,*† Juergen Theuer,* Erdenechimeg Shagdarsuren,* Eva Kaergel,† Horst Honeck,† Joon-Keun Park,‡ Marija Markovic,* Eduardo Barbosa-Sicard,† Ralf Dechend,* Maren Wellner,* Torsten Kirsch,‡ Anette Fiebeler,* Michael Rothe,§ Hermann Haller,‡ Friedrich C. Luft,*† and Wolf-Hagen Schunck†

From HELIOS Klinikum-Berlin, Franz Volhard Clinic, and Medical Faculty of the Charité, Humboldt University of Berlin, Berlin; the Max Delbrück Center for Molecular Medicine,† Berlin-Buch; the Department of Medicine-Nephrology,‡ Hannover Medical School, Hannover; and FILT GmbH,§ Berlin-Buch, Germany*

Cytochrome P450 (CYP)-dependent arachidonic acid (AA) metabolites are involved in the regulation of renal vascular tone and salt excretion. The epoxygenation product 11,12-epoxyeicosatrienoic acid (EET) is anti-inflammatory and inhibits nuclear factor-κB activation. We tested the hypothesis that the peroxisome proliferator-activated receptor-α-activator fenofibrate (Feno) induces CYP isoforms, AA hydroxylation, and epoxygenation activity, and protects against inflammatory organ damage. Double-transgenic rats (dTGRs) overexpressing human renin and angiotensinogen genes were treated with Feno. Feno normalized blood pressure, albuminuria, reduced nuclear factor-κB activity, and renal leukocyte infiltration. Renal epoxygenase activity was lower in dTGRs compared to nontransgenic rats. Feno strongly induced renal CYP2C23 protein and AA-epoxygenase activity under pathological and nonpathological conditions. In both cases, CYP2C23 was the major isoform responsible for 11,12-EET formation. Moreover, we describe a novel CYP2C23-dependent pathway leading to hydroxy-EETs (HEETs), which may serve as endogenous peroxisome proliferator-activated receptor-α activators. The capacity to produce HEETs via CYP2C23-dependent epoxygenation of 20-HETE and CYP4A-dependent hydroxylation of EETs was reduced in dTGR kidneys and induced by Feno. These results demonstrate that Feno protects against angiotensin II-induced renal damage and acts as inducer of CYP2C23-mediated epoxygenase activities. We propose that CYP-dependent EET/HEET production may serve as an anti-inflammatory control mechanism. ***(Am J Pathol 2004, 164:521–532)***

Arachidonic acid (AA) is metabolized by cytochrome P450 (CYP) systems to several oxygenated metabolite classes with potent biological activities.[1] Major metabolites in the kidney include 20- and 19-hydroxyeicosatetraenoic acid (20- and 19-HETE) and four regioisomeric epoxyeicosatrienoic acids (5,6-, 8,9-, 11,12-, and 14,15-EETs). Numerous studies have implicated these CYP-dependent AA-metabolites in the regulation of renal function and vascular tone.[2–5] Both 20-HETE and the EETs promote salt excretion. A deficiency in tubular expression of 20-HETE-generating CYP4A enzymes, as well as a failure to up-regulate EET-generating CYP2C enzymes, was related to salt-sensitive hypertension in Dahl rats.[4,6,7] 20-HETE also serves as an endogenous vasoconstrictor. Inhibition of 20-HETE generation reduced blood pressure in spontaneously hypertensive rats[8] and DOCA salt-treated rats.[9] EETs act as vasodilators and may function as endothelium-derived hyperpolarizing factors.[10–12] Furthermore, Node and colleagues[13] showed that EETs have anti-inflammatory properties in endothelial cells inhibiting cytokine-induced activation of the nuclear transcription factor kappa B (NF-κB).

Peroxisome proliferator-activated receptor (PPAR)-α activators, such as clofibrate and fenofibrate (Feno) lower triglycerides, but also influence CYP-dependent AA metabolism. Fibrates induce CYP4A gene expression via a PPAR-α response element in the promoter region.[14] Fibrates reduce blood pressure in salt-sensitive Dahl rats,[15,16] in stroke-prone spontaneously hypertensive rats,[16] and in DOCA salt-hypertensive mice.[17] Roman and colleagues[4,15] suggested that enhanced tubular CYP4A expression and 20-HETE formation are involved in this process. PPAR-α activators also prevent the activation of inflammatory response genes by inhibiting NF-κB and activator protein-1 signaling.[18]

Supported by the Deutsche Forschungsgemeinschaft (Mu1467/1-1 and Schu822/3-1), the Klinischer-Pharmakologischer Verbund Berlin-Brandenburg, and the European Union.

Accepted for publication October 20, 2003.

Address reprint requests to Dominik N. Muller, Franz-Volhard-Clinic at MDC, Wiltberg Strasse 50, 13125 Berlin, Germany. E-mail: mueller@fvk-berlin.de.

We have studied double-transgenic rats (dTGRs) harboring the human genes for renin and angiotensinogen. dTGRs develop hypertension and profound renal damage.[19–22] NF-κB and activator protein-1 activation and associated consequences are important features of this model.[19,20,22] We recently showed that dTGRs exhibit significantly decreased renal AA epoxygenase activities and that the expression of the predominant EET-generating CYP-isoform, CYP2C23, is progressively lost in renal cortical tubules.[23] Therefore, decreased EET production might be involved in mediating hypertension and inflammatory end-organ damage. We examined whether or not the PPAR-α activator Feno is able to restore the CYP-dependent renal AA metabolism, reduce inflammatory responses, and protect against angiotensin (Ang) II-induced renal damage.

Materials and Methods

Experimental Animals

Rats overexpressing the human renin and angiotensinogen genes [dTGR(hREN L10*hAOGEN L1623)]; abbreviated in the following as (dTGRs) have been described in detail earlier.[19–23] dTGRs were purchased from RCC Ltd. (Füllinsdorf, Switzerland). Experiments were conducted in age-matched 4-week-old male untreated dTGRs (n = 20), Feno-treated dTGRs (n = 11; 30 mg/kg/day in the diet from weeks 4 to 7), and nontransgenic Sprague-Dawley rats (SD) (n = 7; Tierzucht Schönwalde, Germany) after due approval (permit no. G 408/97). To investigate the effect of Feno on the expression of CYP isoforms and their activities under nonpathological conditions, we treated in an additional protocol SD with the same dose of Feno and normal chow (n = 6 each). Systolic blood pressure was measured by tail-cuff under light ether anesthesia. Urine samples were collected throughout 24 hours. Urinary albumin was measured by enzyme-linked immunosorbent assay (CellTrend, Luckenwalde, Germany). All rats were killed at age 7 weeks.

TaqMan Polymerase Chain Reaction (PCR)

Real-time quantitative reverse transcriptase (RT)-PCR was performed using the TaqMan system (PE Biosystems) as described earlier in detail.[22] Each sample was in triplicate. For quantification, the target sequence (n = 6 each group) was normalized in relation to the β-actin product. The sequences were: β-actin-F: TCCTGGCCTCACTGTCCAC; β-actin-R: GGGCCGGACTCATCGTACT; β-actin-P: 6-FAM-TTCCAGCAGATGTGGATCAGCAAGCA-TAMRA; human angiotensinogen-F: TGAAGAAACTGTCTCCCCGG; human angiotensinogen-R: TCATAAGATCCTTGCAGCACCA; human angiotensinogen-P: 6-FAM-CCATCCACCTGACCATGCCCCA-TAMRA; human renin-F: CGAGAAAGCCTGAAGGAACG; human renin-R: TCATGGGTTGGCTCCACTC; human renin-P: 6-FAM-TGGACATGGCCAGGCTTGGTCC-TAMRA; CYP2C23-F: ACCGAGACAACCAGCACCA; CYP2C23-R: TGGCTTGCACCTCTGGATACT; CYP2C23-P: 6-FAM-CCTGAGATTCGGGCTCCTGCTGCTCCTTAT-TAMRA.

Immunohistochemistry

Ice-cold acetone-fixed cryosections (6 μm) were stained by immunofluorescence and alkaline phosphatase anti-alkaline phosphatase technique as described earlier.[19,20,23] The sections were incubated with the following monoclonal antibodies: anti-CD4 (PharMingen, Heidelberg, Germany), anti-ED-1, anti-CD8 (all Serotec, Germany), anti-CD86, anti-Ox62, and anti-Ox6 MHC II (all BD Pharmigen, Germany), and polyclonal antibodies: anti-CYP2C23,[7] anti-CYP4A1 (Daiichi Pure Chemicals, Tokyo, Japan), and anti-fibronectin (Paesel, Frankfurt, Germany), and anti-collagen IV (Southern Biotechnology, Birmingham, AL). Cy3 and fluorescein-isothiocyanate secondary antibodies (Dianova, Hamburg, Germany) were used for co-localization stainings. Semiquantitative scoring of infiltrated cells and matrix expression was performed as described earlier.[20] Fifteen different cortical areas of each kidney (n = 5 in all groups) were analyzed. For quantification of perivascular macrophage infiltration, all selected view fields included a small vessel in their analysis. Quantification of $CD4^+$ T cells, MHC II+ cells, and CD86+ cells was performed periglomerular, whereas CD8+ cells were quantified interstitially. The samples were examined without knowledge of the rats' identity. Two independent observers who were unaware of the treatments assessed collagen IV and fibronectin expression. The data are expressed in arbitrary units (0 to 5) based on the staining intensity.

Electrophoretic Mobility Shift Assay

Tissue preparation for electrophoretic mobility shift assay was performed as described earlier.[19] Nuclear extracts (5 μg protein) from whole kidneys were incubated in binding reaction medium with 0.5 ng of ^{32}P-dATP end-labeled oligonucleotide, containing the NF-κB-binding site from the MHC enhancer (H2K, 5′-gatcCAGGGCTGGGGATTCCCCATCTCCACAGG). Unlabeled H2K oligonucleotides (50 ng) were used in competition assays. Antibodies for supershift analysis (p50 and p65) were obtained from Santa Cruz, Germany.

Renal Microsomal AA Metabolism

Microsomes were prepared from freshly dissected kidneys and AA hydroxylase and epoxygenase activities were determined as described previously.[23] Briefly, renal microsomes (80 μg of protein in a total volume of 0.1 ml) were incubated in 50 mmol/L Tris/HCl buffer, pH 7.5, with 10 nmol [1-^{14}C] AA (0.55×10^6 dpm; final concentration, 100 μmol/L) in the presence of NADPH (0.5 mmol/L) for 20 minutes at 37°C. In immunoinhibition experiments, microsomes were preincubated for 30 minutes at 37°C with 100 μg/ml of rabbit IgG (125 μg IgG/mg microsomal protein) before substrate and NADPH were added. Anti-CYP2C23 IgG[7] concentrations were varied between 0

and 100 μg/ml whereas the total amount of IgG was kept constant by appropriate additions of control rabbit IgG. AA hydroxylase activities were determined as the sum of 19- and 20-HETE and AA epoxygenase activities as the sum of EETs and corresponding dihydroxyeicosatrienoic acids (DHETs) produced per minute and mg of microsomal protein. To analyze the formation of secondary AA metabolites, renal microsomes were incubated under the standard reaction conditions described above using AA (56 mCi/mmol) and primary metabolites (19-HEET, 20-HETE, EETs, and DHETs) in a final concentration of 20 μmol/L.

Western Blot Analysis

Microsomal protein (15 μg per lane) was separated on 10% sodium dodecyl sulfate-polyacrylamide gel electrophoresis and immunoblotting was performed as we have described previously.[23] Primary antibodies used were goat antisera against rat CYP4A1 (reacts with all CYP4A isoforms) and rat CYP2C11 (both Daiichi Pure Chemicals Co.), and a rabbit IgG against rat CYP2C23.[7]

Oxidation of Primary Metabolites by Recombinant CYP Enzymes

The cDNAs for CYP2C23 and Cyp4a12 were generated by RT-PCR from rat and mouse kidney RNA samples as to be described in detail elsewhere. Recombinant baculoviruses were produced using the Bac-to-Bac System of Gibco-BRL. The recombinant baculovirus for CYP4A1 was kindly provided by Dr. M. L. Schwartzman, New York Medical College, Valhalla, NY. Co-expression of individual CYP isoforms with human NADPH-CYP reductase (CPR) was achieved by co-infection of *Spodoptera frugiperda* (Sf9) cells with the respective recombinant baculoviruses as described previously.[24] Sf9 microsomes containing the recombinant CYP/CPR-systems (10 pmol of CYP2C23 or CYP4A1) were preincubated for 5 minutes at 37°C with different [1-^{14}C]-labeled substrates (2 nmol) in 100 mmol/L of potassium phosphate buffer, pH 7.2 (total volume, 0.1 ml). Reactions were started by addition of NADPH (final concentration, 0.5 mmol/L) and performed at 37°C for 20 minutes.

Preparation of Metabolites

Radiolabeled 20-HETE was produced by hydroxylation of [1-^{14}C]-AA (56 mCi/mmol; Amersham Pharmacia-Biotech) with recombinant Cyp4a12. The reactions were performed in 100 mmol/L of potassium phosphate buffer, pH 7.2, for 20 minutes at 37°C and contained per ml 20 nmol of AA (56 mCi/mmol), 50 pmol of recombinant Cyp4a12 and NADPH (0.5 mmol/L). After extraction with ethyl acetate, the total hydroxylation product was collected from RP-HPLC and further resolved into 19- and 20-HETE by normal phase (NP)-HPLC as described.[17] Radiolabeled EETs and hydroxy-EETs (HEETs) were synthesized by chemical oxidation of [1-^{14}C]-AA (56 mCi/mmol) and 20-HETE (supplemented with trace amounts of [1-^{14}C] 20-HETE; Cayman Chemical), respectively, with m-chloroperoxybenzoic acid.[25,26] 14,15-EET was directly isolated from RP-HPLC. The further EET regioisomers were resolved by NP-HPLC on Nucleosil 100-5 (250 × 4 mm; Macherey-Nagel, Düren, Germany) using hexane:2-propanol:acetic acid (99.5:0.4:0.1, v/v/v) at a flow rate of 1.5 ml/min (11,12-EET, Rt = 12.5 minutes; 8,9-EET, Rt = 16.5 minutes; 5,6-EET, Rt = 24 minutes). HEET regioisomers were resolved by NP-HPLC using a linear gradient from hexane:2-propanol:acetic acid (99.4:0.5:0.1,v/v/v) to hexane:2-propanol:acetic acid (96.4:3.5:0.1, v/v/v) for 60 minutes at a flow rate of 1 ml/min.

LC-MS Analysis

The HPLC equipment consisted of Agilent HP 1100 series with binary pump, autosampler with thermostat, photodiode array detector, and atmospheric pressure ionization mass spectrometry detector. The analysis was done on an analytical column Zorbax Eclipse XDB-C8, 4.6 × 150 mm [time] 5 μm. Five μl of ethanolic solution of the HEETs was injected. The gradient elution was started with a mobile phase 30:70 (v/v) mixture of acetonitrile/ammonium acetate buffer (0.01 mol/L, pH = 8.5) and a flow rate of 0.4 ml/minute. Acetonitrile was increased throughout 15 minutes to 90% and held for 10 minutes. The drying gas flow was 11 l/minute and drying gas temperature 350°C. Capillary voltage was 3000 V and fragmentor voltage was 60 V. The detection was made in negative mode between m/z = 200 to 400.

Statistical Analysis

Data are presented as means ± SEM. Statistically significant differences in mean values were tested by analysis of variance, repeated measures when appropriate, and the Scheffé test. Mortality was examined with a Kaplan-Meier analysis. A value of $P < 0.05$ was considered statistically significant. The data were analyzed using Statview statistical software.

Results

Feno Reduces Mortality, Systolic Blood Pressure, and Renal Damage

In untreated male dTGRs, 10 of 20 rats died before sacrifice, whereas Feno treatment reduced mortality to zero ($P < 0.001$). No nontransgenic SD rat died before the end of the study. Blood pressure progressively increased in untreated dTGRs and exceeded that of SD control rats more than 100 mm Hg at week 7 (213 ± 3 mm Hg *versus* 107 ± 3 mm Hg; $P < 0.001$). Feno-treated dTGRs remained normotensive and had blood pressure values of 120 ± 3 mm Hg at week 7 not different from SD control rats (Figure 1A). Urinary albumin excretion was markedly higher in dTGRs than in SD rats: 29.3 ± 3.1 mg/day *versus* 0.19 ± 0.04 mg/day ($P < 0.001$). Feno-

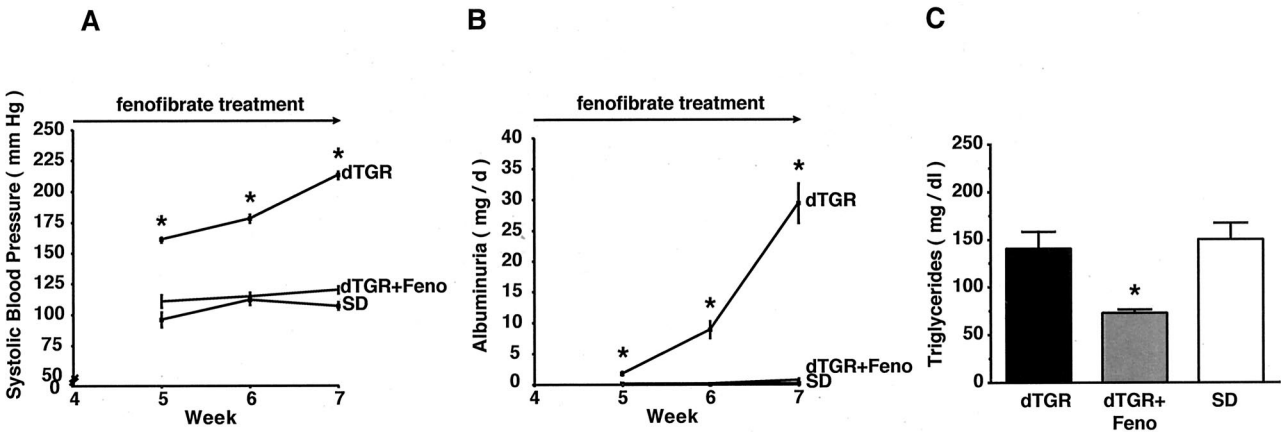

Figure 1. Feno-treated dTGRs are compared to untreated dTGRs and SD controls. **A:** Systolic blood pressure was higher ($P < 0.001$) in untreated dTGRs than in Feno-treated dTGRs and in SD. **B:** Untreated dTGRs showed increased 24-hour albuminuria compared to SD ($P < 0.001$), whereas Feno-treated dTGRs were not different from SD. **C:** Feno-treated dTGRs showed decreased plasma triglycerides compared to untreated dTGRs and SD ($P < 0.05$).

treated dTGRs did not develop significant albuminuria (0.7 ± 0.26 mg/day; Figure 1B). Plasma triglyceride levels from untreated dTGRs and SD were not different (140 ± 17 mg/dl *versus* 151 ± 17 mg/dl; $P = 0.89$). Feno-treated dTGRs showed significantly decreased levels (73 ± 3 mg/dl; Figure 1C). Feno had dramatic effects on matrix protein deposition. Collagen IV (Figure 2A) and fibronectin (data not shown) staining in Feno-treated dTGRs were reduced almost to the levels observed in SD rats. Untreated dTGRs, on the other hand, showed prominent staining for these matrix proteins (grade 1+ for Feno-treated dTGRs *versus* 5+ for vehicle-treated dTGRs *versus* 1+ for SD rats, respectively). To analyze whether or not Feno action on end-organ protection was because of down-regulation of one of the transgenes, we performed TaqMan RT-PCR for human renin and angiotensinogen. Renal renin and liver angiotensinogen expression was statistically not different between dTGRs and Feno-treated dTGRs; no signal was observed in nontransgenic SD (for renin: 51 ± 23 *versus* 43 ± 12 *versus* 0.05 ± 0.03; for angiotensinogen: 29 ± 3 *versus* 25 ± 5 *versus* 0.004 ± 0.002 arbitrary units, respectively).

Effect of Feno on Renal Inflammation and NF-κB Activity

Feno abolished inflammatory response, as well as infiltration of immune cells in the kidney. Monocytes/macrophages (ED-1+) infiltrated predominantly around the damaged vessels, whereas T-helper cells (CD4+) showed perivascular and interstitial and cytotoxic T cells (CD8+) interstitial, periglomerular, and glomerular locations (not shown). Semiquantification of ED-1+, CD4+, and CD8+ T-cell infiltration showed a significant reduction of these cells in the kidney after chronic Feno treatment ($P < 0.001$; Figure 2B). In addition, Feno also reduced dendritic cell, MHC II+ cell, and CD86+ cell infiltration toward nontransgenic levels ($P < 0.001$; Figure 2B). These data suggest that immunocompetent cell activation was markedly suppressed by fibrate treatment.

We next studied transcription factor activation in renal tissue with electrophoretic mobility shift assay. Four vehicle-treated dTGRs (Figure 3) showed markedly increased NF-κB DNA binding activity, whereas four Feno-treated dTGRs showed activity that was little different from SD controls. Antibodies directed against the p50 and p65 subunits of NF-κB resulted in supershifts. Thus, Feno treatment reduced NF-κB activation in dTGRs. We also analyzed the effect of Feno on NF-κB DNA binding and NF-κB-dependent promoter activity in tubular epithelial NRK-52E cells. Two hours of Feno preincubation not only reduced tumor necrosis factor-α-induced NF-κB DNA-binding activity significantly, but also reduced NF-κB-dependent promoter activity more than 80% (data not shown).

CYP-Dependent AA Metabolism and Immunoinhibition of AA-Epoxygenase Activities

Renal microsomes of dTGRs showed a significantly reduced AA epoxygenase activity (Figure 4A). The production of EETs was decreased to 61% and reached only 130 ± 21 pmol/minute/mg compared to 214 ± 15 pmol/minute/mg in SD controls ($P < 0.05$; Figure 4A). Feno treatment strongly induced the AA-epoxygenase activity to 249 ± 19 pmol/minute/mg. This value was nearly twofold higher than in untreated dTGRs ($P < 0.01$) and exceeded that of SD controls. In contrast, Feno did not increase hydroxylase activity (Figure 4B). We were next interested in the CYP isoforms that were responsible for EET formation in dTGRs and Feno-treated renal microsomes. An antibody directed against CYP2C23 dose-dependently decreased the AA epoxygenase activities more than 90% in both groups (Figure 4C). In contrast, AA-hydroxylase activities were not inhibited.

Effect of Feno on CYP Expression

The CYP2C23 content of dTGR renal microsomes was moderately diminished compared to SD. Feno treatment

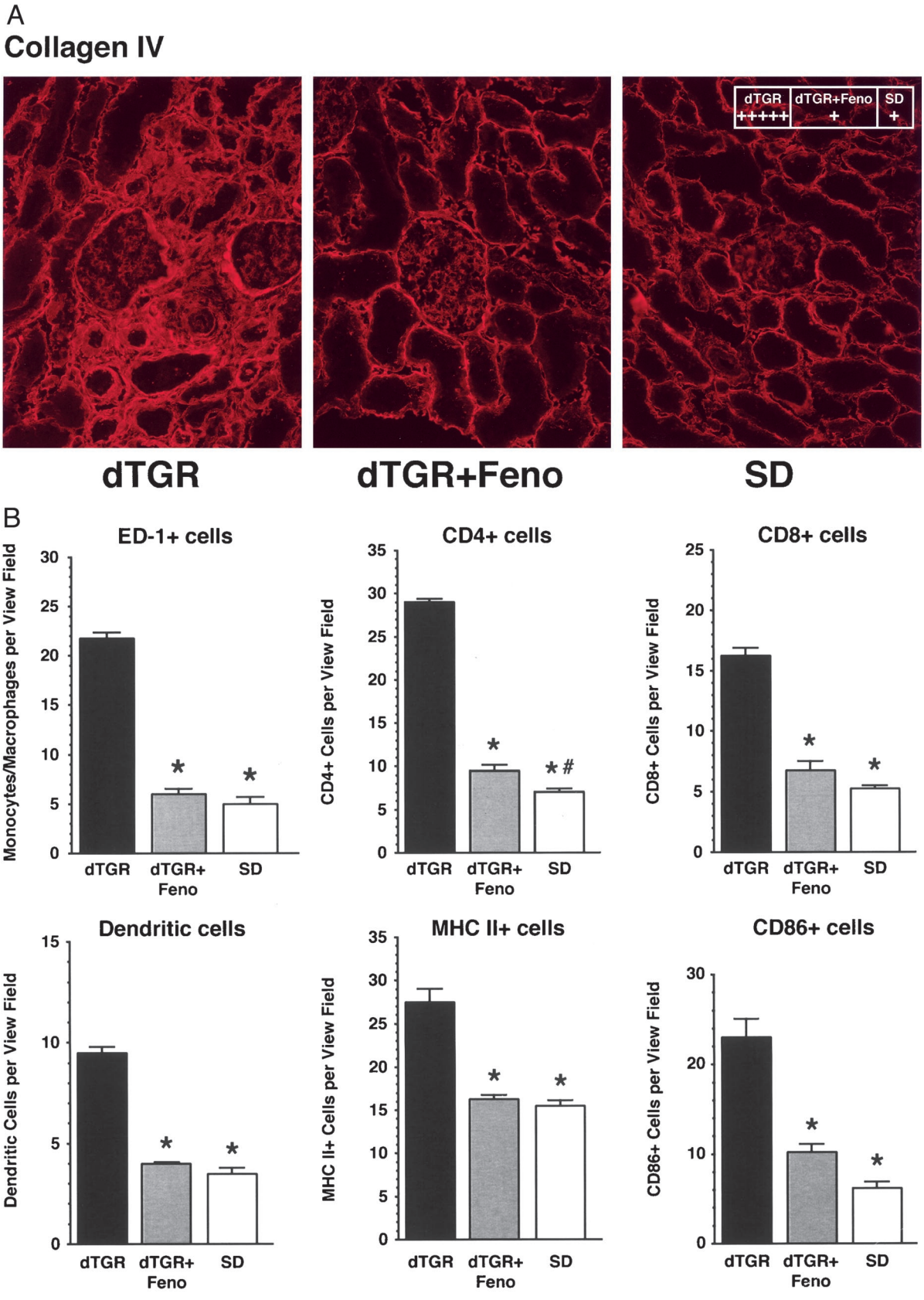

Figure 2. A: Feno treatment reduced renal collagen IV expression toward SD level. **B:** Feno suppresses immunocompetent cell infiltration. Untreated dTGR kidneys showed increased infiltration of ED-1+, $CD4^+$, and CD8+ T cells, dendritic cells, MHC II+, and CD86+ cells. Semiquantification ($n = 5$ per group) showed that Feno reduced ED-1+, CD8+, dendritic cells, MHC II+, and CD86+ cells to nontransgenic level, while $CD4^+$ T-cell infiltration was slightly higher than to SD ($P < 0.05$). Results are mean ± SEM (*, $P < 0.05$ dTGR *versus* dTGR+Feno and SD).

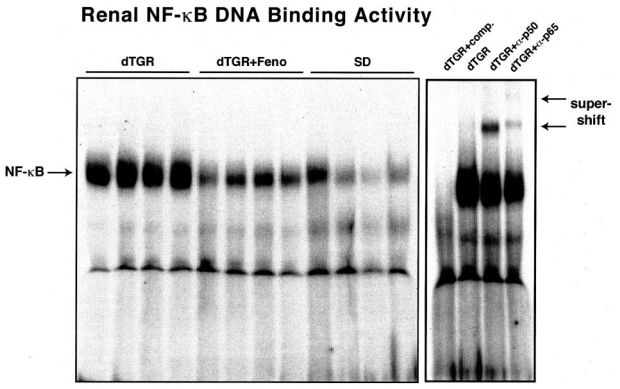

Figure 3. Renal NF-κB DNA-binding activity. DNA-binding activity for NF-κB was markedly induced in dTGRs. Nontransgenic SD showed little NF-κB activity. Feno reduced NF-κB activity toward SD levels. Competition and supershift experiments with antibodies against p50 and p65 showed specificity of the NF-κB activity.

significantly increased CYP2C23 in dTGRs ($P < 0.001$), corresponding to 167 ± 13% of the SD control ($P < 0.001$) (Figure 4D). TaqMan RT-PCR analysis showed that renal CYP2C23 mRNA levels were not changed (0.9 ± 0.1 arbitrary units for Feno-treated dTGRs *versus* 1.1 ± 0.2 for untreated dTGRs *versus* 1.0 ± 0.1 for SD rats, respectively) suggesting a posttranscriptional regulation. CYP2C11 protein levels were dramatically decreased in dTGR renal microsomes to 15 ± 2% of SD control values ($P < 0.001$) and were only weakly induced by Feno treatment (Figure 4D). CYP4A protein was almost identical in renal microsomes of untreated dTGRs and SD control rats. Feno treatment resulted in a strong induction of CYP4A proteins to ~180% compared to samples from untreated dTGRs ($P < 0.001$; Figure 4D).

We performed immunohistochemical analysis to further localize renal CYP2C23 expression. Untreated dTGRs showed reduced renal CYP2C23 expression. Feno treatment of dTGRs resulted in abundant CYP2C23 expression in cortical tubules (Figure 5A), collecting ducts, and outer medullary tubules (data not shown) indistinguishable from SD kidneys. CYP4A proteins were expressed in all outer medullary tubules, some cortical tubules and in most tubules along the medullary rays. CYP4A staining was more pronounced in Feno-treated dTGRs compared with untreated dTGRs and SD (Figure 5B). In addition, dTGR kid-

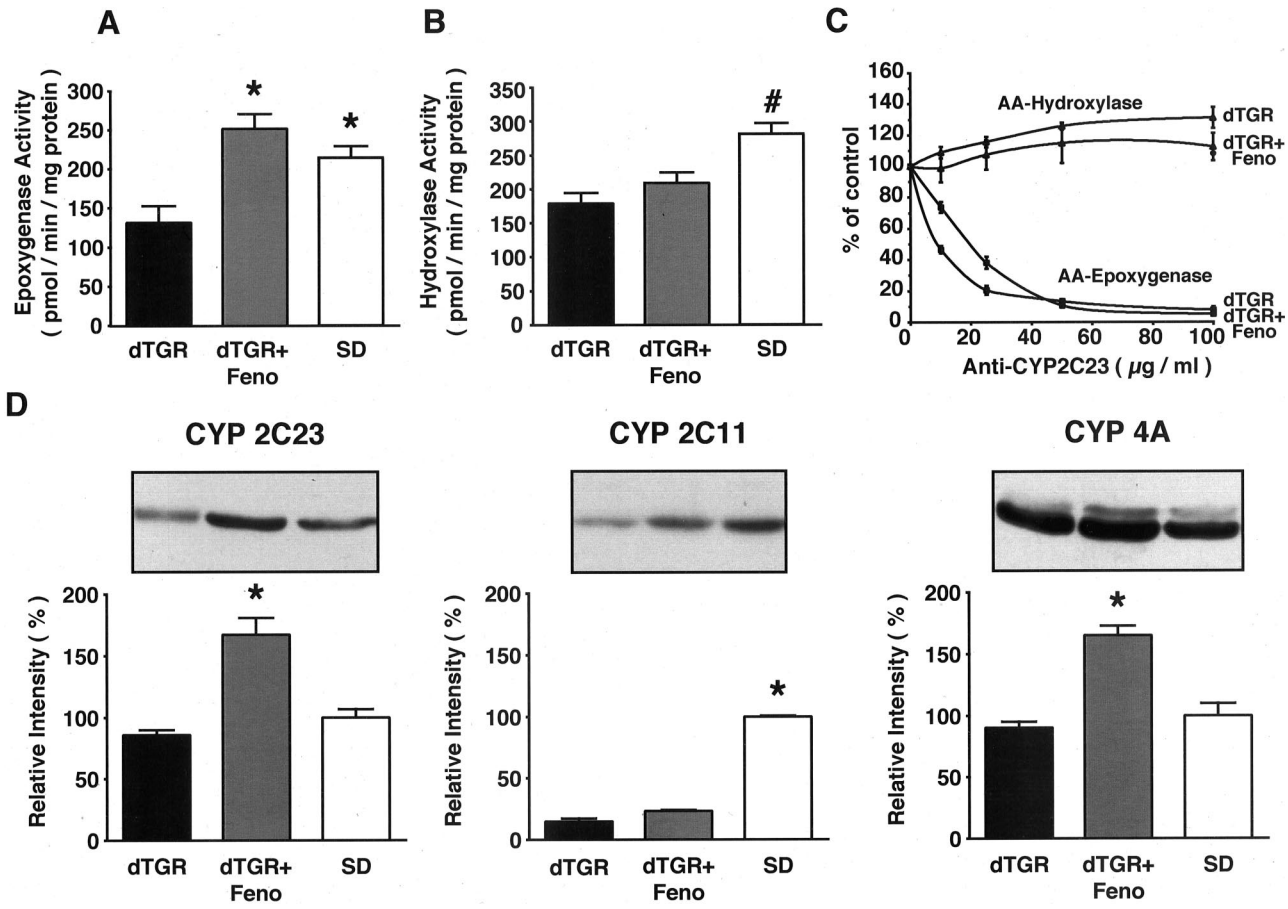

Figure 4. A: AA epoxygenase activities of renal microsomes isolated from untreated and Feno-treated dTGRs were compared to microsomes from SD. Untreated dTGRs had lower epoxygenase activities compared to Feno-treated dTGRs ($P < 0.01$) and SD ($P < 0.05$). **B:** AA hydroxylase activities were not induced by Feno and remained below SD levels. Results are mean ± SEM (*, $P < 0.05$ dTGRs *versus* dTGR+Feno and SD; ≠, $P < 0.05$ SD *versus* dTGR and dTGR+Feno). **C:** Effect of anti-CYP2C23 IgG on CYP-dependent AA hydroxylation and epoxygenation by renal dTGR and Feno-dTGR microsomes ($n = 4$ in both groups). The activity of the respective sample containing only control IgG was set at 100%. **D:** Western blot analysis of renal microsomes showed that CYP2C23 protein level was augmented in Feno-treated dTGRs ($n = 9$) compared to untreated dTGRs ($n = 6$) and SD ($n = 8$) ($P < 0.001$). CYP2C11 protein level was reduced in untreated and Feno-treated dTGRs compared to SD ($P < 0.001$). Feno treatment of dTGRs resulted in increased levels for CYP4A ($P < 0.001$). Results are mean ± SEM and percentage of SD.

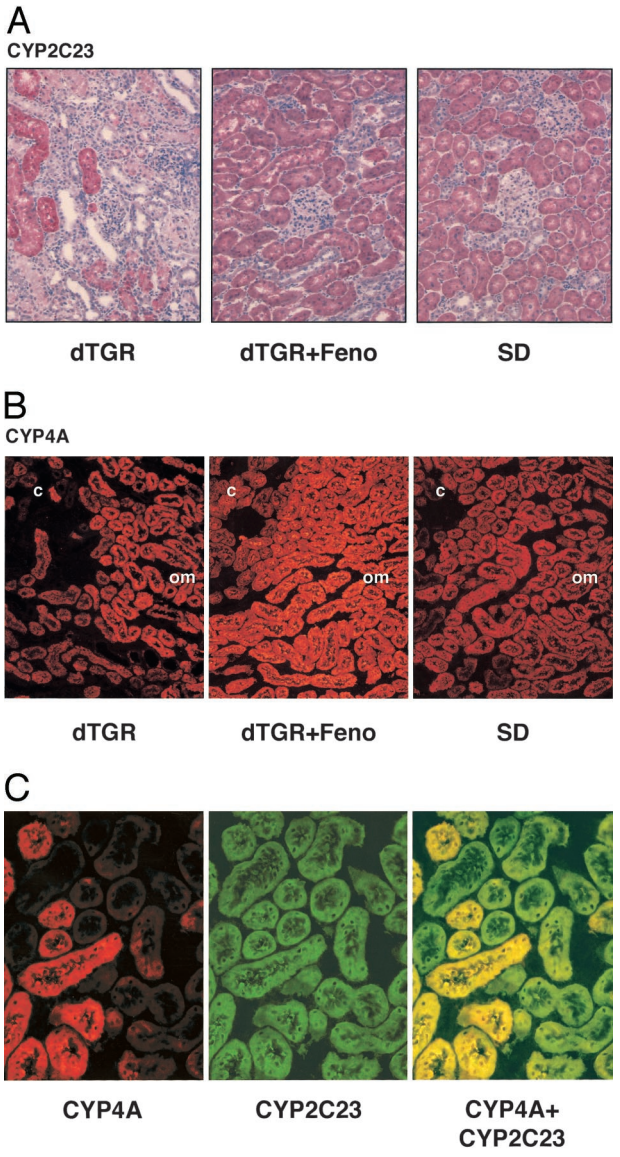

Figure 5. A: CYP2C23 immunoreactivity in cortical tubules. In kidneys with minor damage most of the tubules showed immunoreactivity. In contrast, in untreated dTGRs with severe renal damage >50% of tubules showed no staining. **B:** Feno-treated dTGRs showed increased CYP4A immunoreactivity compared to untreated dTGRs and SD. The photomicrographs show sections of the border between outer medulla (om) and cortex (c). **C:** Renal cortical section showed co-localization of CYP4A (red) and CYP2C23 (green) and the merged picture (orange).

ney showed less CYP4A immunoreaction in areas with tubular damage. We next stained both CYP isoforms in the same section of a nontransgenic rat and found that CYP4A (red) and CYP2C23 (green) were co-localized in certain cortical tubules (Figure 5C), tubules along medullary rays, and outer medullary tubules (data not shown).

Effects of Feno on CYP-Dependent AA Metabolism under Physiological Conditions

To elucidate the effects of fibrates under physiological conditions, we treated nontransgenic SD rats with Feno. Chronic Feno treatment did not affect systolic blood pressure (108 ± 3 mm Hg *versus* 113 ± 3 mm Hg, $P = 0.29$) or albuminuria (0.12 ± 0.02 mg/day *versus* 0.11 ± 0.01 mg/day; $P = 0.71$; SD+Feno *versus* SD.). Feno reduced plasma triglycerides (72 ± 3 mg/dl *versus* 142 ± 19 mg/dl; $P < 0.05$; SD+Feno *versus* SD.). Feno treatment had a profound influence on CYP-dependent AA metabolism in SD rats. Epoxygenase activity was significantly induced and reached 530 ± 25 pmol/minute/mg compared to 190 ± 11 pmol/minute/mg in SD controls (Figure 6A). In contrast, hydroxylase activity showed only a nonsignificant tendency to increased values after Feno treatment (237 ± 12 pmol/minute/mg *versus* 204 ± 17 pmol/minute/mg; Figure 6B). Neutralizing CYP2C23 antibodies clearly inhibited the formation of epoxygenase products both in untreated and Feno-treated SD rats (Figure 6C). Western blotting revealed significantly increased microsomal CYP2C23, CYP2C11, and CYP4A protein levels after Feno treatment (161 ± 13%, 150 ± 17%, and 256 ± 46% of SD controls, respectively; Figure 6E).

CYP-Dependent Generation of Secondary AA Metabolites

All AA epoxygenase and hydroxylase assays described above were performed at an AA concentration of 100 μmol/L to favor the formation of primary products (19-/20-HETE and EETs/DHETs). To analyze the generation of secondary metabolites, we used a lower AA concentration (20 μmol/L). Two additional product peaks with retention times of ~9.0 and 4.5 minutes were clearly detectable under these conditions (Figure 7A). Taking the sum of these two product peaks, secondary metabolite generation was approximately fivefold less in renal microsomes from dTGRs compared to SD rats (Figure 7B). Feno treatment induced secondary metabolite generation sixfold in dTGRs and 3.5-fold in SD rats (Figure 7B). The 9-minute products co-migrated with chemically epoxidized 20-HETE (hydroxy-EETs; HEETs) and those at 4.5 minutes with hydrolyzed HEETs (hydroxy-DHETs; HDHETs).

To clarify the origin of the secondary AA metabolites, we analyzed the metabolism of 20-HETE and of EETs by renal microsomes. As shown in Figure 7C, both 20-HETE and 11,12-EET were directly converted to products with a retention time of 9 minutes in NADPH-dependent reactions. 20-HETE epoxygenase and 11,12-EET hydroxylase activities were strongly induced in Feno-treated compared with SD microsomes (394 ± 17 pmol/minute/mg *versus* 128 ± 8 pmol/minute/mg and 364 ± 5 pmol/minute/mg *versus* 183 ± 4 pmol/minute/mg, respectively, $P < 0.001$; Figure 6D). Moreover, HEETs were efficiently produced incubating 20-HETE with recombinant CYP2C23 or EETs with recombinant CYP4A1 (Figure 7D). HDHETs were directly produced by renal microsomes using 11,12-DHET as substrate (Figure 7C). HEET fractions were collected during RP-HPLC and further resolved into regioisomers by NP-HPLC (Figure 7E). To prepare suitable standard compounds, we took advantage of the high regioselectivity of CYP4A1.[26] The metabolites produced by ω-hydroxylation of 8,9-, 11,12- and

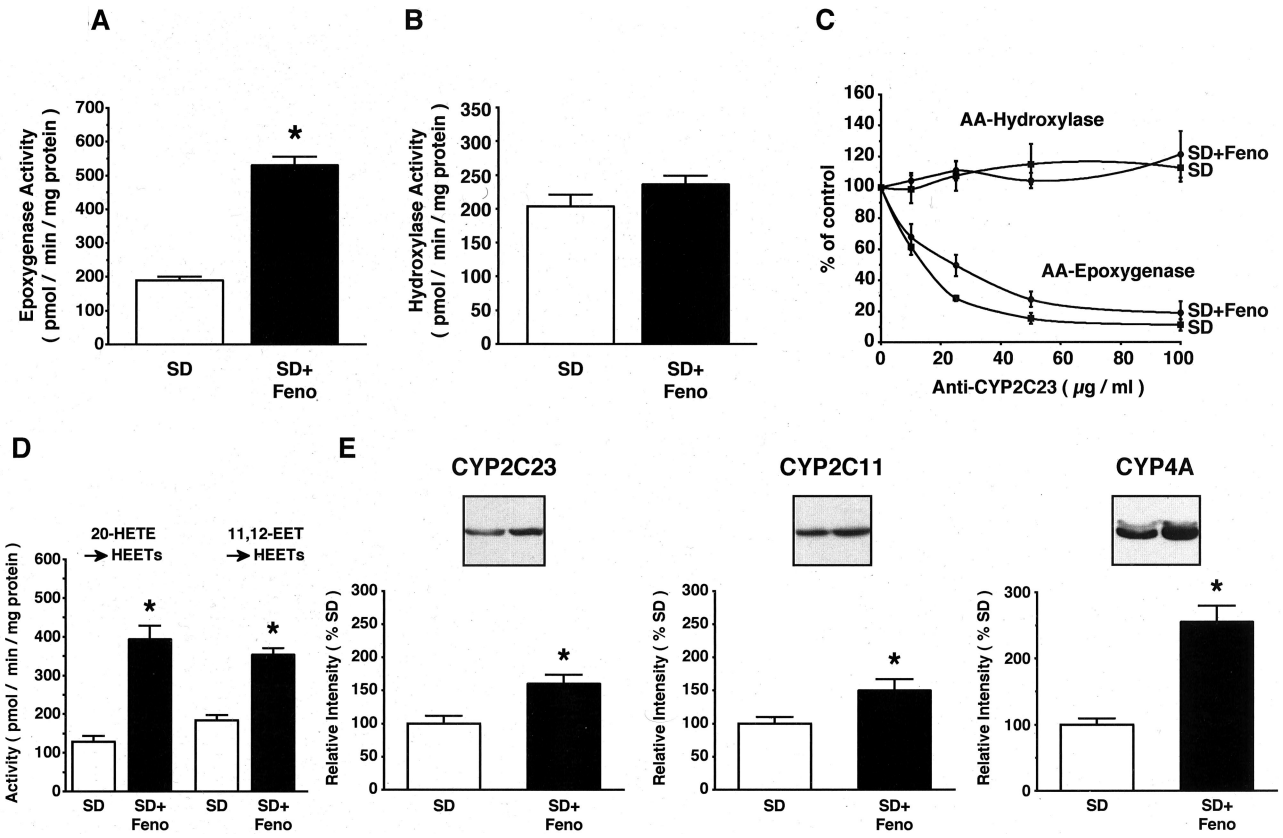

Figure 6. Effect of Feno on CYP-dependent AA metabolism in SD rats. **A** and **B:** Epoxygenase activity was induced in Feno-treated SD, while hydroxylase activity was unchanged after Feno treatment. Results are mean ± SEM ($n = 6$ each; *, $P < 0.05$ SD *versus* SD+Feno). **C:** Quantification of CYP2C23 immunoinhibition experiments. Anti-CYP2C23 antibodies in both groups (compare with Figure 4C) abolished AA-epoxygenase activity. **D:** Renal microsomes from Feno-treated SD rats showed increased 20-HETE epoxygenase and 11,12-EET hydroxylase activities compared with SD. Results are mean ± SEM ($n = 6$ each; *, $P < 0.01$ SD *versus* SD+Feno). **E:** Western blotting revealed increased microsomal CYP2C23, CYP2C11, and CYP4A protein levels after Feno treatment. Results are mean ± SEM and are percent of untreated SD (*, $P < 0.05$ SD *versus* SD+Feno).

14,15-EET with recombinant CYP4A1 showed retention times of 44.9 minutes (20-hydroxy-8,9-EET; 20,8,9-HEET), 44.0 minutes (20,11,12-HEET), and 53.7 minutes (20,14,15-HEET) in NP-HPLC (nomenclature as described in Cowart and colleagues[26]). Epoxygenation of 20-HETE by recombinant CYP2C23 resulted in a major product co-migrating with 20,8,9-HEET (~80% of total product) and a minor product co-migrating with 20,14,15-HEET (Figure 7E). 20,11,12-HEET occurred only in trace amounts (less than 3% of total product). The identity of these products was confirmed by LC-MS analyses in which the CYP2C23-generated metabolites of 20-HETE showed a predominant peak at m/z 335 corresponding to the expected molecular mass (M-1) of HEETs (Figure 7F). A very similar HEET pattern with 20,8,9-HEET as the predominant metabolite was obtained after incubation of renal microsomes with 20-HETE (Figure 7E). Conversion of 19-HETE by recombinant CYP2C23 yielded products with a retention time of 38.5 minutes in NP-HPLC probably representing an unresolved mixture of 19-hydroxy-8,9-EET and 11,12-EET (data not shown). The HEET fraction after conversion of AA with renal microsomes from

Figure 7. Primary and secondary products of CYP-dependent renal microsomal AA metabolism. **A:** Representative RP-HPLC chromatograms showing the conversion of AA (20 μmol/L) by renal microsomes isolated from the different animal groups indicated. **B:** Experiments are summarized ($n = 5$ per group). The data represent the total amounts (in pmol) of individual product classes formed during 20 minutes of incubation using 80 μg of microsomal protein in 0.1-ml reaction mixtures. **C:** Conversion of 11,12-EET, 20-HETE, and 11,12-DHET to HEETs and HDHETs by renal microsomes (80 μg per 0.1 ml reaction mixture) isolated from Feno-treated SD. Reactions were performed at a substrate concentration of 20 μmol/L for 20 minutes in the presence of an epoxide hydrolase inhibitor (dicyclohexylurea; 5 μmol/L). None of the substrates was converted in the absence of NADPH. The sum of HEETs and HDHETs produced represented 25% (11,12-EET conversion), 46% (20-HETE conversion), and 35% (11,12-DHET) of the total radioactivities applied. **D:** Formation of HEETs by conversion of 8,9-EET with recombinant CYP4A1 and of 20-HETE with recombinant CYP2C23. Twenty-three percent (8,9-EET by CYP4A1) and 43% (20-HETE by CYP2C23) of the introduced substrates (2 nmol in a total reaction volume of 0.1 ml) were converted to HEETs by 10 pmol of recombinant CYP enzymes in 20 minutes. Control microsomes isolated from Sf9 cells only expressing the NADPH-CYP reductase, but no CYP2C23, did not convert 20-HETE. **E:** Resolution of HEET regioisomers by NP-HPLC. HEET fraction produced during incubation of renal microsomes with AA (**top**, y-scale*2) consisted of 19-hydroxy-EETs (product peak 1), 20,11,12-HEET (peak 2), 20,8,9-HEET (peak 3, major product), and 20,14,15-HEET (peak 4). Recombinant CYP2C23 (**middle**) and renal microsomes (**bottom**) epoxidized 20-HETE to 20,8,9-HEET (major product) and 20,14,15-HEET, whereas 20,11,12-HEET occurred only in trace amounts. The *y* axis of all HPLC chromatograms represents the response of the radioactivity monitor (1 V corresponds to $5*10^4$ cpm). **F:** LC-MS analysis of the HEET regioisomers produced by CYP2C23-catalyzed epoxygenation of 20-HETE. 20-HETE supplemented with trace amounts of [1-^{14}C] 20-HETE was converted with recombinant CYP2C23. The total HEET fraction produced was collected from RP-HPLC and an aliquot (200 pmol) was further resolved by LC-MS. HEET fractions consisted of 20,14,15-HEET (peak at 11.6 minutes), 20,11,12-HEET (12.0 minutes), and 20,8,9-HEET (major product, 12.3 minutes). The mass spectra of all three compounds showed a predominant peak at m/z 335 (shown in the **inset** for 20,8,9-HEET) corresponding to the expected molecular mass (M-1) of HEETs.

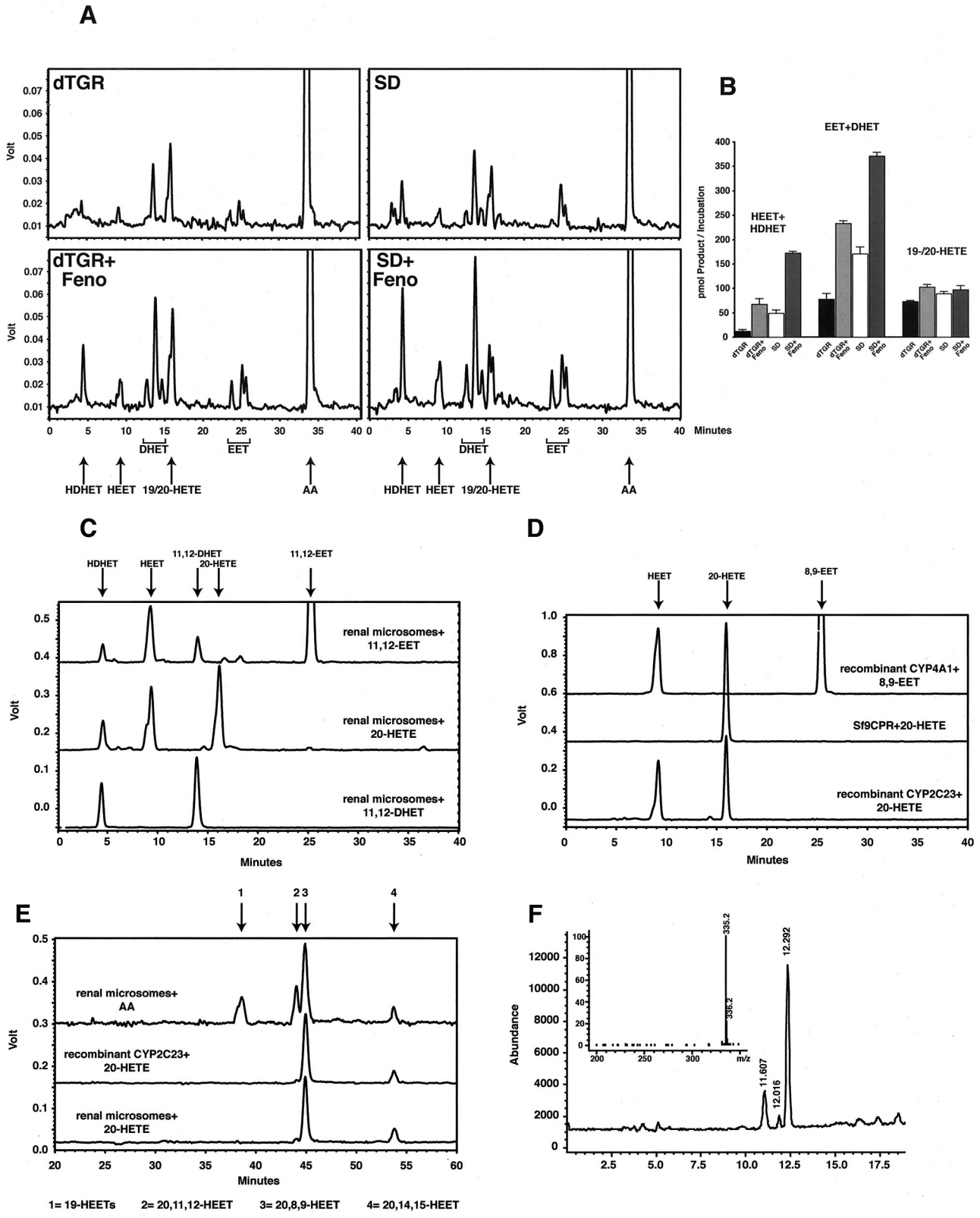
A
dTGR
SD
dTGR+ Feno
SD+ Feno
Volt
Minutes
DHET
EET
HDHET
HEET
19/20-HETE
AA
B
EET+DHET
HEET+ HDHET
19-/20-HETE
pmol Product / Incubation
C
HDHET
HEET
11,12-DHET
20-HETE
11,12-EET
renal microsomes+ 11,12-EET
renal microsomes+ 20-HETE
renal microsomes+ 11,12-DHET
D
HEET
20-HETE
8,9-EET
recombinant CYP4A1+ 8,9-EET
Sf9CPR+20-HETE
recombinant CYP2C23+ 20-HETE
E
renal microsomes+ AA
recombinant CYP2C23+ 20-HETE
renal microsomes+ 20-HETE
1= 19-HEETs
2= 20,11,12-HEET
3= 20,8,9-HEET
4= 20,14,15-HEET
F
Abundance
335.2
336.2
m/z
11.607
12.016
12.292

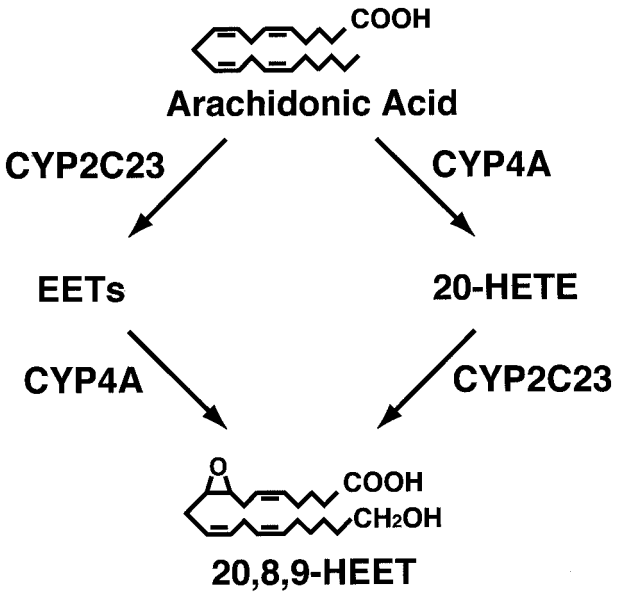

Figure 8. Schematic representation of CYP-dependent renal AA metabolism including the novel role of CYP2C23 in the production of HEETs. Only the structure of 20,8,9-HEET is given which represents the main product of CYP2C23-catalyzed 20-HETE epoxygenation. Further potential regioisomers involve 20,5,6-, 20,11,12-, and 20,14,15-HEET and a similar set of metabolites derived from 19-HETE. EET stands for a mixture 8,9-, 11,12-, and 14,15-EET produced from AA by CYP2C23 in a ratio of 24:61:15.[7] The CYP4A-isoforms predominantly expressed in the male rat kidney prefer 11,12-EET as substrate[26] for HEET formation. In renal microsomes, both pathways contribute to HEET generation as indicated by the occurrence of 20,8,9- and 20,11,12-HEET as products of AA conversion (compare Figure 7).

Feno-treated SD rats was resolved into four product peaks migrating at 38.5 minutes (19-hydroxy-EETs; 21% of total product), 44.0 minutes (20,11,12-HEET; 21%), 44.9 minutes (20,8,9-HEET; 50%), and 53.7 minutes (20,14,15-HEET; 8%).

Discussion

We studied the effect of the PPAR-α activator Feno on CYP-dependent AA-metabolism and on Ang II-induced renal damage. Feno protected dTGRs from hypertension and inflammatory end-organ damage. Because untreated dTGRs and SD rats showed similar plasma triglyceride levels, we believe that the reno-protective effect was triglyceride-independent. We provide the first data that PPAR-α activation induced renal CYP2C23-dependent AA-epoxygenase activity under pathological and nonpathological conditions. CYP2C23 activity not only determined the formation of anti-inflammatory EETs, but also the metabolism of 20-HETE to HEETs providing a novel route for the generation of these recently discovered endogenous PPAR-α activators.[26]

Renal damage in dTGRs is a result of uncontrolled inflammation triggered by high local Ang II concentrations.[19–21] We showed previously that end-organ damage and hypertension are primarily independent processes in dTGRs. Blood pressure reduction with inhibitors not affecting Ang II generation did not reverse end-organ damage.[21] In contrast, anti-inflammatory and immunosuppressive treatment protected against renal damage in dTGRs despite elevated blood pressure levels.[19,20] A similar organ-protective effect in dTGRs was only achieved by specific inhibition of RAS with ACE inhibitors and AT1-receptor antagonists. The beneficial effects of Feno obviously did not result from reduced Ang II levels because the expression of the transgenes for human renin and angiotensinogen on Feno-treatment was unchanged.

The present finding that Feno abolished the activation of NF-κB in dTGRs suggests that PPAR-α activation represses renal inflammation already at a very early stage. The prevention of leukocyte infiltration and activation of immunocompetent cells, as well as reduction in albuminuria, is probably a consequence of proinflammatory transcription factor inhibition. Direct anti-inflammatory mechanisms of PPAR-α activation were recently identified by *in vitro* studies. The mechanisms involve protein-protein interactions between PPAR-α and the p65 and c-Jun subunits of NF-κB and activator protein-1, respectively, and an induction of the inhibitory protein IκBα that retains NF-κB in a cytoplasmic inactive complex.[27,28]

Our finding that renal CYP-dependent EET and HEET generation are down-regulated in dTGRs and strongly induced on Feno-treatment points to additional mechanisms that may have contributed to the strong anti-inflammatory effect of the PPAR-α activator. EETs are able to inhibit cytokine-induced activation of the IκB kinase complex, a key step in the pathway leading to NF-κB activation.[13] Our immunoinhibition experiments revealed that CYP2C23 represented the predominant renal AA epoxygenase in dTGRs and SD rats, as well as in the corresponding Feno-treated groups. CYP2C23 has a regioselectivity in favor of producing 11,12-EET,[7] the most potent anti-inflammatory regioisomer.[13]

Cowart and colleagues[26] showed that HEETs function as high-affinity endogenous PPAR-α activators. Our data indicate that the capacity to produce HEETs is very low in dTGRs compared to SD rats and is strongly induced in both Feno-treated dTGRs and Feno-treated SD rats. The ability of CYP4A enzymes to hydroxylate EETs to HEETs has been already reported.[26] We found a novel pathway, in which HEETs are efficiently produced by CYP2C23-dependent epoxygenation of 20-HETE. HEET generation via both pathways required an interaction of CYP4A and CYP2C enzymes (Figure 8). Therefore, alterations in their activities alter the AA metabolites formation. Pathophysiological CYP2C down-regulation, as found in our dTGRs model, may lead to: 1) reduced EET levels, 2) even more pronounced decrease in HEET production, and 3) presumably also to accumulation of 20-HETE levels because of a lower rate of CYP2C-catalyzed 20-HETE epoxygenation. CYP2C23 produced predominantly 20,8,9-HEET, which was also the main HEET regioisomer formed in renal microsomal AA metabolism. This result suggests that CYP2C23-dependent 20-HETE epoxygenation is a major route of HEET production. According to our immunohistochemical analysis, CYP4A and CYP2C23 are co-localized in most medullary and certain cortical tubules and may thus indeed co-operate to produce HEETs. In this context, Feno appears as a substitute for the decreased endogenous HEET levels in dTGRs and to trig-

ger a positive feedback involving enhanced CYP-dependent formation of the endogenous PPAR-α activators.

The mechanisms regulating CYP2C23 expression and activity are primarily unknown. We found that down-regulation of CYP2C23 activity in dTGRs is indeed Ang II-dependent. Renal microsomal epoxygenase activity could be restored to the SD rat level by treating dTGRs with blockers of the renin-angiotensin system (unpublished data). Moreover, a recent study performed with SD rats demonstrated that Ang II-infusion results in reduced renal CYP2C23 protein levels and EET generation.[29] We were surprised to find that Feno treatment strongly enhanced CYP2C23 protein levels and CYP2C23-dependent epoxygenase activity in dTGRs and SD rats. The promoter of the CYP2C23 gene does not contain a typical PPAR-α response element.[30] Further excluding a direct transcriptional regulation, we found that the renal CYP2C23 mRNA levels were not different between dTGRs and SD rats and were not influenced by Feno treatment. Interestingly, high-salt intake of rats also induced CYP2C23 at a posttranscriptional level.[7]

The fact that Feno not only protected against renal damage, but also against the development of Ang II-induced hypertension may be because of elevated EET generation. The anti-hypertensive effect of EETs is generally attributed to their ability to increase renal blood flow and to promote salt excretion.[1,2,4,5,31] EETs act as endothelium-derived hyperpolarizing factors in a number of vascular beds including renal arterioles.[10–12,31] In addition, proinflammatory mediators decrease endothelial CYP2C expression and endothelium-derived hyperpolarizing factor formation.[32] In preglomerular arterioles, vasoconstriction in response to Ang II is enhanced when Ang II-stimulated EET generation is abolished.[31,33] Thus, decreased EET levels in dTGRs potentiate Ang II-induced vasoconstriction and salt reabsorption. We speculate that Feno enhanced EET generation and thereby counterregulated vasoconstriction and salt reabsorption. Supporting this view, soluble epoxide hydrolase inhibition, which also increases renal EET levels, reduced hypertension in Ang II-infused rats.[34] The effect of Feno on AA-hydroxylase activities was less pronounced, although we found a significant induction of CYP4A protein levels. Thus, increased tubular 20-HETE production, that was held responsible for the anti-hypertensive effect of fibrates in Dahl salt-sensitive rats and in spontaneously hypertensive rats, appears to play a minor role in our model.[3,15,16]

We believe that fibrate-mediated blood pressure reduction is a common action in rodents. PPAR-α activation reduced blood pressure not only in our transgenic model, but also in Dahl salt-sensitive rats,[15,16] spontaneously hypertensive rats rats,[16] and Ang II-infused SD rats.[35] Fibrates showed anti-inflammatory properties in humans;[36] however, the effect on blood pressure is less clear. Some studies demonstrated a blood pressure-lowering effect with Feno,[37] gemfibrozil,[38] and bezafibrate,[39] while others did not.[38] PPAR-α activation by fibric acids improves insulin sensibility, and decreases thrombosis and vascular inflammation. PPAR-α activators decrease the risk of coronary heart disease in patients with normal low-density lipoprotein cholesterol and low high-density lipoprotein-cholesterol,[40] they slow the progression of premature coronary atherosclerosis,[41] particularly in patients with type 2 diabetes.[42]

Taken together, prevention of end-organ damage in dTGRs by Feno provided *in vivo* evidence for a protective effect through PPAR-α activation. In addition to the inhibitory effect of PPAR-α agonists on NF-κB signaling, increased generation of anti-inflammatory EETs may have contributed to Feno actions. Moreover, induction of CYP2C23 activity not only increased EETs, but also the endogenous PPAR-α activator HEET. We propose that increased EET/HEET levels are important factors protecting against Ang II-induced hypertension and organ damage. Stimulation of CYP-dependent AA-epoxygenation as demonstrated in the present study and decreased EET inactivation by inhibiting the soluble epoxide hydrolase may provide attractive therapeutic targets for the future.

Acknowledgments

We thank May-Britt Köhler, Mathilde Schmidt, Ramona Zummach, and Christel Andrée for excellent technical assistance; Dr. Jorge H. Capdevila (Vanderbilt University, Nashville, TN) for providing the antibodies against CYP2C23; and Dr. Michal L. Schwartzman (New York Medical College, Valhalla, NY) for providing the CYP4A1-baculovirus.

References

1. Capdevila JH, Falck JR, Harris RC: Cytochrome P450 and arachidonic acid bioactivation. Molecular and functional properties of the arachidonate monooxygenase. J Lipid Res 2000, 41:163–181
2. Zeldin DC: Epoxygenase pathways of arachidonic acid metabolism. J Biol Chem 2001, 276:36059–36062
3. Roman RJ, Alonso-Galicia M, Wilson TW: Renal P450 metabolites of arachidonic acid and the development of hypertension in Dahl salt-sensitive rats. Am J Hypertens 1997, 10:63S–67S
4. Roman RJ: P-450 metabolites of arachidonic acid in the control of cardiovascular function. Physiol Rev 2002, 82:131–185
5. McGiff JC, Quilley J: 20-HETE and the kidney: resolution of old problems and new beginnings. Am J Physiol 1999, 277:R607–R623
6. Makita K, Takahashi K, Karara A, Jacobson HR, Falck JR, Capdevila JH: Experimental and/or genetically controlled alterations of the renal microsomal cytochrome P450 epoxygenase induce hypertension in rats fed a high salt diet. J Clin Invest 1994, 94:2414–2420
7. Holla VR, Makita K, Zaphiropoulos PG, Capdevila JH: The kidney cytochrome P-450 2C23 arachidonic acid epoxygenase is upregulated during dietary salt loading. J Clin Invest 1999, 104:751–760
8. Wang MH, Zhang F, Marji J, Zand BA, Nasjletti A, Laniado-Schwartzman M: CYP4A1 antisense oligonucleotide reduces mesenteric vascular reactivity and blood pressure in SHR. Am J Physiol 2001, 280:R255–R261
9. Oyekan AO, McAward K, Conetta J, Rosenfeld L, McGiff JC: Endothelin-1 and CYP450 arachidonate metabolites interact to promote tissue injury in DOCA-salt hypertension. Am J Physiol 1999, 276: R766–R775
10. Quilley J, McGiff JC: Is EDHF an epoxyeicosatrienoic acid? Trends Pharmacol Sci 2000, 21:121–124
11. Fisslthaler B, Popp R, Kiss L, Potente M, Harder DR, Fleming I, Busse R: Cytochrome P450 2C is an EDHF synthase in coronary arteries. Nature 1999, 401:493–497
12. Campbell WB, Gauthier KM: What is new in endothelium-derived

hyperpolarizing factors? Curr Opin Nephrol Hypertens 2002, 11:177–183
13. Node K, Huo Y, Ruan X, Yang B, Spiecker M, Ley K, Zeldin DC, Liao JK: Anti-inflammatory properties of cytochrome P450 epoxygenase-derived eicosanoids. Science 1999, 285:1276–1279
14. Johnson EF, Palmer CN, Griffin KJ, Hsu MH: Role of the peroxisome proliferator-activated receptor in cytochrome P4504A gene regulation. EMBO J 1996, 10:1241–1248
15. Roman RJ, Ma YH, Frohlich B, Markham B: Clofibrate prevents the development of hypertension in Dahl salt-sensitive rats. Hypertension 1993, 21:985–988
16. Shatara RK, Quest DW, Wilson TW: Fenofibrate lowers blood pressure in two genetic models of hypertension. Can J Physiol Pharmacol 2000, 78:367–371
17. Honeck H, Gross V, Erdmann B, Kaergel E, Neunaber R, Milia AF, Schneider W, Luft FC, Schunck WH: Cytochrome P450-dependent renal arachidonic acid metabolism in desoxycorticosterone acetate-salt hypertensive mice. Hypertension 2000, 36:610–616
18. Delerive P, Fruchart JC, Staels B: Peroxisome proliferator-activated receptors in inflammation control. J Endocrinol 2001, 169:453–459
19. Muller DN, Heissmeyer V, Dechend R, Hampich F, Park JK, Fiebeler A, Shagdarsuren E, Theuer J, Elger M, Pilz B, Breu V, Schroer K, Ganten D, Dietz R, Haller H, Scheidereit C, Luft FC: Aspirin inhibits NF-kappaB and protects from angiotensin II-induced organ damage. EMBO J 2001, 15:1822–1824
20. Muller DN, Shagdarsuren E, Park JK, Dechend R, Mervaala E, Hampich F, Fiebeler A, Ju X, Finckenberg P, Theuer J, Viedt C, Kreuzer J, Heidecke H, Haller H, Zenke M, Luft FC: Immunosuppressive treatment protects against angiotensin II-induced renal damage. Am J Pathol 2002, 161:1679–1693
21. Mervaala E, Muller DN, Schmidt F, Park JK, Gross V, Bader M, Breu V, Ganten D, Haller H, Luft FC: Blood pressure-independent effects in rats with human renin and angiotensinogen genes. Hypertension 2000, 35:587–594
22. Muller DN, Mervaala EM, Dechend R, Fiebeler A, Park JK, Schmidt F, Theuer J, Breu V, Mackman N, Luther T, Schneider W, Gulba D, Ganten D, Haller H, Luft FC: Angiotensin II (AT(1)) receptor blockade reduces vascular tissue factor in angiotensin II-induced cardiac vasculopathy. Am J Pathol 2000, 157:111–122
23. Kaergel E, Muller DN, Honeck H, Theuer J, Shagdarsuren E, Mullally A, Luft FC, Schunck WH: P450-dependent arachidonic acid metabolism and angiotensin II-induced renal damage. Hypertension 2002, 40:273–279
24. Lauterbach B, Barbosa-Sicard E, Wang MH, Honeck H, Kaergel E, Theuer J, Schwartzman ML, Haller H, Luft FC, Gollasch M, Schunck WH: Cytochrome P450-dependent eicosapentaenoic acid metabolites are novel BK channel activators. Hypertension 2002, 39:609–613
25. Falck JR, Yadagiri P, Capdevila J: Synthesis of epoxyeicosatrienoic acids and heteroatom analogs. Methods Enzymol 1990, 187:357–364
26. Cowart AL, Wei S, Hsu MH, Johnson EF, Krishna MU, Falck JR, Capdevila JH: The CYP 4A isoforms hydroxylate epoxyeicosatrienoic acids to form high affinity PPAR ligands. J Biol Chem 2002, 277: 35105–35112
27. Delerive P, De Bosscher K, Besnard S, Vanden Berghe W, Peters JM, Gonzalez FJ, Fruchart JC, Tedgui A, Haegeman G, Staels B: Peroxisome proliferator-activated receptor alpha negatively regulates the vascular inflammatory gene response by negative cross-talk with transcription factors NF-kappaB and AP-1. J Biol Chem 1999, 274: 32048–32054
28. Delerive P, Gervois P, Fruchart JC, Staels B: Induction of IkappaBalpha expression as a mechanism contributing to the anti-inflammatory activities of peroxisome proliferator-activated receptor-alpha activators. J Biol Chem 2000, 275:36703–36707
29. Zhao X, Pollock DM, Zeldin DC, Imig JD: Salt-sensitive hypertension after exposure to angiotensin is associated with inability to upregulate renal epoxygenases. Hypertension 2003, 42:775–780
30. Roussel F, Marie S, Cresteil T: Gene structure and promoter analysis of the rat constitutive CYP2C23 gene. DNA Cell Biol 1995, 14:777–788
31. Imig JD: Eicosanoid regulation of the renal vasculature. Am J Physiol 2000, 279:F965–F981
32. Kessler P, Popp R, Busse R, Schini-Kerth VB: Proinflammatory mediators chronically downregulate the formation of the endothelium-derived hyperpolarizing factor in arteries via a nitric oxide/cyclic GMP-dependent mechanism. Circulation 1999, 99:1878–1884
33. Arima S, Endo Y, Yaoita H, Omata K, Ogawa S, Tsunoda K, Abe M, Takeuchi K, Abe K, Ito S: Possible role of P-450 metabolite of arachidonic acid in vasodilator mechanism of angiotensin II type 2 receptor in the isolated microperfused rabbit afferent arteriole. J Clin Invest 1997, 100:2816–2823
34. Imig JD, Zhao X, Capdevila JH, Morisseau C, Hammock BD: Soluble epoxide hydrolase inhibition lowers arterial blood pressure in angiotensin II hypertension. Hypertension 2002, 39:690–694
35. Diep QN, Amiri F, Touyz RM, Cohn JS, Endemann D, Neves MF, Schiffrin EL: PPARalpha activator effects on Ang II-induced vascular oxidative stress and inflammation. Hypertension 2002, 40:866–871
36. Staels B, Koenig W, Habib A, Merval R, Lebret M, Torra IP, Delerive P, Fadel A, Chinetti G, Fruchart JC, Najib J, Maclouf J, Tedgui A: Activation of human aortic smooth-muscle cells is inhibited by PPARalpha but not by PPARgamma activators. Nature 1998, 393: 790–793
37. Idzior-Walus B, Sieradzki J, Rostworowski W, Zdzienicka A, Kawalec E, Wojcik J, Zarnecki A, Blane G: Effects of comicronised fenofibrate on lipid and insulin sensitivity in patients with polymetabolic syndrome X. Eur J Clin Invest 2000, 30:871–878
38. Wierzbicki AS: Lipid lowering: another method of reducing blood pressure? J Hum Hypertens 2002, 16:753–760
39. Jonkers IJ, de Man FH, van der Laarse A, Frolich M, Gevers Leuven JA, Kamper AM, Blauw GJ, Smelt AH: Bezafibrate reduces heart rate and blood pressure in patients with hypertriglyceridemia. J Hypertens 2001, 19:749–755
40. Bloomfield Rubins H, Davenport J, Babikian V, Brass LM, Collins D, Wexler L, Wagner S, Papademetriou V, Rutan G, Robins SJ: Reduction in stroke with gemfibrozil in men with coronary heart disease and low HDL cholesterol: the Veterans Affairs HDL Intervention Trial (VA-HIT). Circulation 2001, 103:2828–2833
41. Ericsson CG, Hamsten A, Nilsson J, Grip L, Svane B, de Faire U: Angiographic assessment of effects of bezafibrate on progression of coronary artery disease in young male postinfarction patients. Lancet 1996, 347:849–853
42. Vakkilainen J, Steiner G, Ansquer JC, Aubin F, Rattier S, Foucher C, Hamsten A, Taskinen MR: Relationships between low-density lipoprotein particle size, plasma lipoproteins, and progression of coronary artery disease: the Diabetes Atherosclerosis Intervention Study (DAIS). Circulation 2003, 107:1733–1737